

# CONFINEMENT IDENTITY EXPERIMENTS IN ASDEX UPGRADE AND JET

**K. Thomsen**<sup>1</sup>, R. Budny<sup>3</sup>, J.P. Christiansen<sup>1</sup>, J.G. Cordey<sup>1</sup>, J.C. Fuchs<sup>2</sup>, O. Gruber<sup>2</sup>,  
S. de Pena Hempel<sup>2</sup>, G. Huysmans<sup>1</sup>, P. Lomas<sup>1</sup>, F. Ryter<sup>2</sup>, G. Sadler<sup>1</sup>, H. Salzmann<sup>2</sup>,  
J. Schmeizner<sup>2</sup>, H.B. Schunke<sup>1</sup>, J. Stober<sup>2</sup>, W. Suttrop<sup>2</sup> and B. Tubbing<sup>1</sup>

<sup>1</sup>*JET Joint Undertaking, Abingdon OX14 3EA UK*

<sup>2</sup>*ASDEX Upgrade Team, IPP, D-85748 Garching, Germany*

<sup>3</sup>*Princeton Plasma Physics Laboratory, New Jersey 08540, USA*

## 1. Scale invariance of confinement

Many experiments carried out on Tokamaks such as JET, TFTR, DIII, Alcator, PLT and ASDEX have been devoted to studies of the scaling of confinement with dimensionless parameters like normalised Larmor radius  $\rho_*$ , collisionality  $\nu_*$ , and  $\beta$ . The use of dimensionless parameters is based on the scale invariance principle formulated by Kadomtsev and Connor-Taylor [1]. This principle starts from the use of confinement models for local diffusivity  $\chi$  expressed as

$$\chi = \chi_B F(\rho_*, \nu_*, \beta, q_\psi, \varepsilon, \kappa \dots) \quad (1)$$

where  $\chi_B = T/B$  is the Bohm diffusivity i.e. no dependence on radiation or atomic physics. The global analogue of (1) expresses the confinement time  $\tau_E$  as

$$B\tau_E = \langle \rho_*^{-2} \rangle / F(\langle \rho_* \rangle, \langle \nu_* \rangle, \beta_N, q_{95}, \varepsilon, \kappa) \quad (2)$$

and (2) involves global averages of the dimensionless parameters in (1). The dimensionless function  $F$  depends on the equation chosen to model confinement (Vlasov, Boltzmann, MHD etc.). The scale invariance principle predicts that the product  $\omega_c \tau_E$  (cyclotron frequency times confinement time) is invariant under any transformation in which  $F$  and its arguments are invariant. To keep  $\rho_*$ ,  $\nu_*$ ,  $\beta$  etc. fixed in such a transformation, e.g. from JET with a minor radius  $a = 0.90\text{m}$  to AUG (ASDEX Upgrade) with  $a = 0.48\text{m}$ , the dimensional parameters like density  $n$ , temperature  $T$ , field  $B$ , current  $I$ , input power  $P$ , must all scale with say minor radius  $a$  as [2]

$$n \sim a^{-2}, \quad T \sim a^{-1/2}, \quad B \sim a^{-5/4}, \quad I \sim a^{-1/4}, \quad P \sim a^{-3/4}. \quad (3)$$

If the variables in (1) chosen to describe confinement are the correct ones then the scale invariance principle implies

$$B\tau_E = \text{const.} \quad \text{or} \quad \tau_E \sim a^{5/4} \quad \text{and} \quad q \sim a^{-11/4} \quad (4)$$

where  $q$  is local heat flux.

A collaboration between JET and AUG has included a series of “Identity experiments” [2] in which plasma configurations on the two tokamaks are produced with identical shapes and identical values of the parameters in (1-2). These identity experiments have featured the following scans:

1. Power scan at a low values of  $na^2$ .
2. Power scan at a higher value of  $na^2$ .
3. Variation of  $q_{95}$ .
4. L→H threshold [3].

In the next two sections we compare the global and local data obtained on the two tokamaks; the experiments have been performed in the ELMy H-mode regime which remains steady for periods longer than 5 sec (JET).

## 2. Global features of Identity pulses

The global operates in Eq. (2) are defined as

$$\langle \rho_* \rangle = \frac{m_e^{1/2}}{\sqrt{6} e \mu_o} \left( \frac{\varepsilon W}{a^3 \kappa n I_\phi^2} \right)^{1/2}, \quad \langle v_* \rangle = 3\sqrt{2}\pi^{5/2} \frac{e^4 \log \Lambda}{\varepsilon_o^2} \frac{a^7 n^3 \kappa^2}{\varepsilon^3 w^2} \quad (5)$$

$$\beta_N = \frac{8}{3} \frac{\varepsilon W}{A I_\phi B_\phi}, \quad q_{95} = \frac{2\pi a^2 B_\phi}{\mu_o R I_\phi} \frac{1 + \kappa^2}{2} \left( 1 + \frac{3}{2} \varepsilon^2 \right)$$

Fig. 1 shows data values for 5 JET low  $n$ , 4 JET high  $n$ , 13 AUG low  $n$ , 1 AUG high  $n$  pulses; the data is time averaged (JET 2 sec, AUG 0.5 sec); symbols J and A refer to JET and AUG respectively, the 5 high  $n$  data points are located at appr.  $\langle \rho_* \rangle \approx 3$ . From both scans we select pairs of “the most identical” pulses for further comparisons. The two sets of JET-AUG pulses that have been selected are shown with large symbols in Fig. 1 as well as in Fig. 2. Fig. 2 demonstrates the global scale invariance for the two high density pulses 43876 (JET), 10712 (AUG) shown in bold as well as for the two low density pulses 43868 (JET), 10343 (AUG): the product  $B_\phi \tau_E$  has approximately the same value for the JET and AUG pulses. These pairs of pulses with identical plasma shapes have nearly identical values of the arguments of  $F$  in (2). It is thus an important result that  $B_\phi \tau_E$  is invariant under the transformation AUG ( $a, n$ ) = (0.48m,  $10^{20} \text{ m}^{-3}$ ) → JET ( $a, n$ ) = (0.90m,  $3.4 \cdot 10^{19} \text{ m}^{-3}$ ).

Both the JET and the AUG pulses have radiation levels  $P_{\text{rad}}/P_{\text{tot}} \sim 25\%$ . For the selected pulses the MHD instabilities (ELM’s, sawteeth) give rise to energy losses  $\sim 25\%$ . However, it can be seen from Fig. 2 that there are two particular JET pulses (low density scan) with

$\langle \rho_* \rangle \approx 5$  where  $B_\phi \tau_E$  value is half the value of the remaining pulses; these two pulses feature intermittent  $n=1$  modes and a continuous  $n=2$  neoclassical tearing mode which strongly degrade their confinement. The ELM and sawtooth frequencies for the selected pulses are (low  $n$ , high  $n$  respectively):

ELM: JET (30,200) Hz, AUG (150, 240) Hz, sawteeth: JET (4,12)Hz, AUG (9,22) Hz.

The ELM frequencies do not follow the frequency scaling  $f a^{-5/4} = \text{const.}$  whereas the sawtooth frequencies do. The amount of energy  $\Delta W_{\text{ELM}}$  lost per ELM is  $\sim 40\text{kJ}$  for the JET low  $n$  pulse; the corresponding power loss  $f_{\text{ELM}} \Delta W_{\text{ELM}}$  becomes  $\sim 1.2\text{MW}$ . For the high  $n$  pulse  $\Delta W_{\text{ELM}}$  is too close to the resolution limit of the diamagnetic loop.

### 3. Profile comparison

The profile measurements of  $T_e$ ,  $T_i$ ,  $n_e$  and calculated heat sources and sinks are mapped onto the square root of the normalised poloidal flux  $x$ . For JET the LIDAR data on  $T_e$  and  $n_e$  is subjected to a further spatial smoothing procedure. Figs. 3, 4 compare the scaled profiles of  $T_e a^{1/2}$  and  $n_e a^2$  for both the low  $n$  and high  $n$  pulses.

It can be seen from Figs. 3 & 4 that the electron temperature and density profiles are very well matched and so too are the ion temperature profiles (not shown). On the other hand Fig. 4 also shows a  $\sim 20\%$  difference in  $na^2$  for the high density pulses. The calculated ion and electron heat fluxes also show different shapes: the deposition profiles are more peaked in JET than in AUG; this applies to both the electron and the ion heat fluxes. Even though the total power losses  $P_e a^{3/4}$  and  $P_i a^{3/4}$  from each channel are matched further identity experiments are needed to confirm that the scale invariance principle applies locally as well as globally.

### References

- [1] B.B. Kadomtsev: Sov. Phys. J. Plasma Physics **1** (1975) 29; J.W. Connor, J.B. Taylor: Nucl. Fus. **17** (1977) 1047.
- [2] K. Lackner: Comments on Plasma Physics and Controlled Fusion **13** (1990) 163.
- [3] W. Suttrop, et al.: "H-mode threshold edge parameter similarity discharges in JET and ASDEX Upgrade", *presented at this conference*.

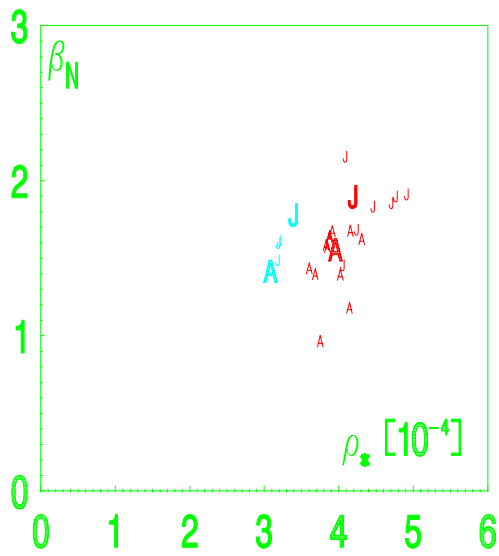


Fig.1 JET (J) and AUG (A) global data matched in both high  $n$  & low  $n$  scans

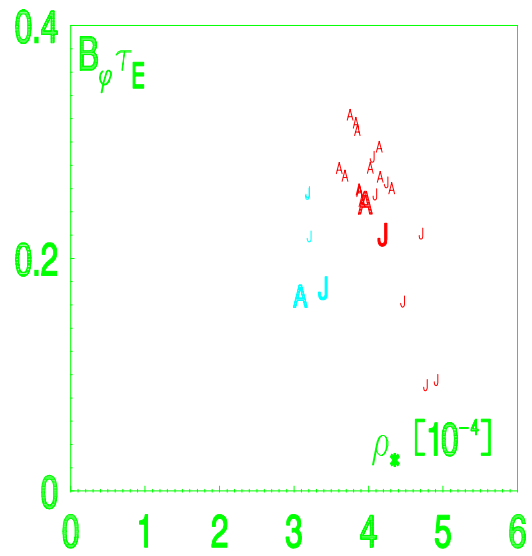


Fig.2 Scale invariance demonstrated for selected pulses (large symbols)

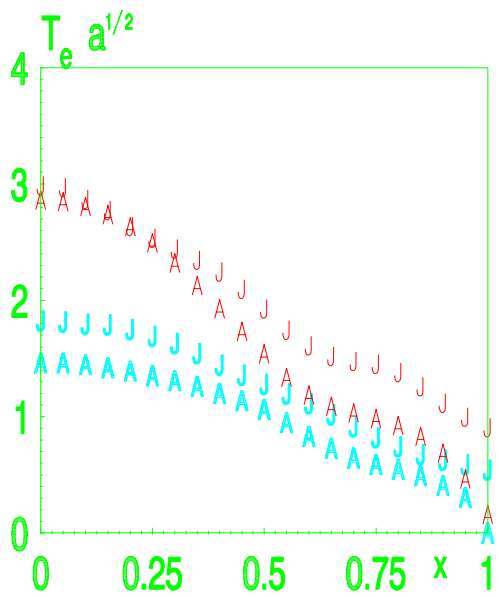


Fig.3 Matching of JET–AUG profiles  
bold: 43876,10712 italic: 43868,10343

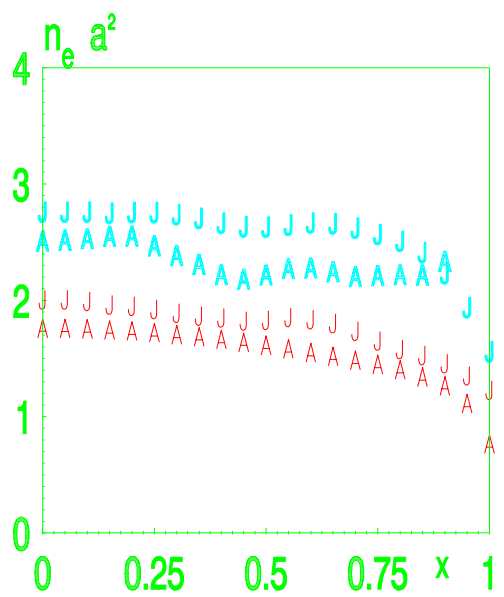


Fig.4 Both high  $n$  and low  $n$  pulses on JET–AUG are well matched